nature methods

BRIEF COMMUNICATION

https://doi.org/10.1038/s41592-020-0770-7

Check for updates

Resolving heterogeneous macromolecular assemblies by Orbitrap-based single-particle charge detection mass spectrometry

Tobias P. Wörner[1,2], Joost Snijder[1,2], Antonette Bennett[3], Mavis Agbandje-McKenna[3], Alexander A. Makarov[1,4] and Albert J. R. Heck[1,2] ✉

We demonstrate single-particle charge detection mass spectrometry on an Orbitrap for the analysis of megadalton biomolecular assemblies. We establish that the signal amplitudes of individual ions scale linearly with their charge, which can be used to resolve mixed ion populations, determine charge states and thus also determine the masses of individual ions. This enables the ultrasensitive analysis of heterogeneous protein assemblies including immunoglobulin oligomers, ribosomes, proteinaceous nanocontainers and genome-packed adeno-associated viruses.

Native mass spectrometry (MS) is a powerful tool, enabling mass analysis of intact macromolecular assemblies in the megadalton range[1]. The exact mass of the intact macromolecular complex is then used to infer its composition and the stoichiometry of subunits, post-translational modifications and ligands bound to the complex[2]. Various mass analyzers, including quadrupole time-of-flight, Fourier-transform ion cyclotron resonance and, most recently, Orbitraps, have all been adapted for native MS experiments[3].

Notably, masses are not measured directly in most MS approaches, but need to be inferred from the mass-to-charge (m/z) ratios of the detected ions. As pioneered by Mann and Fenn[4], the charge states from a population of multiply charged ions generated by electrospray ionization (ESI) can be determined from the m/z values by matching consecutive peaks in the charge state distribution to calculate accurate masses. A general limitation in native MS studies then stems from the fact that the charge state, and thus also the mass, can only be accurately measured when multiple charge states of the same molecular species can be resolved and assigned. This hampers the analysis of larger heterogeneous protein assemblies, such as highly glycosylated proteins, amyloid fibrils, genome-packed viruses and membrane protein complexes decorated with multiple lipid molecules.

Even small variabilities in the monomeric building blocks can result in wide distributions of masses in their larger assemblies. In combination with the often poor desolvation, these broadened mass distributions result in overlapping signals between consecutive charge states, leading to inaccurate mass assignments. A possible solution to these problems is to measure one particle (or ion) at a time, thereby avoiding the convolution of signals that stem from insufficient resolving power[5,6]. When such single-particle detection approaches can be combined with an independent measure of the charge of ions, this opens up the door to bona fide single-particle MS measurements.

Several techniques for single-particle MS capable of determining masses in the megadalton range have emerged, most notably nano electro-mechanical system–MS (NEMS–MS)[7,8] and charge detection–MS (CD–MS)[6,9]. Both NEMS–MS and CD–MS approaches have demonstrated their capability in the analysis of large biomolecular complexes, especially of viruses in the 1–100 MDa range[10–12].

The Orbitrap mass analyzer is sensitive enough to detect single (multiply charged) ions, opening up the possibility for Orbitrap-based single-particle mass analysis[13–15]. It should be noted that single-ion detection was demonstrated much earlier on Fourier-transform ion cyclotron resonance instruments[16]. Following up the early work by Makarov et al. on myoglobin sprayed under denaturing conditions[14], we demonstrated single-ion detection in native MS for the 800 kDa GroEL complex with approximately 70 charges[13]. More recently, Kafader et al.[15] reported that, by stringent filtering of single-ion signals, it is possible to enhance the Orbitrap's resolution by an order of magnitude. Here, we demonstrate that the intensity of a single ion detected in an Orbitrap can be directly used to infer its charge state, enabling Orbitrap-based single-particle MS.

In an Orbitrap (Fig. 1a), the number of charges on an ion determine the amplitude of the induced image current and thereby the intensity of the signal for the corresponding frequency in the mass spectrum recorded. The signal amplitude of a single ion should therefore be a useful proxy to estimate the number of charges it carries, independent of the frequency (that is, m/z) of the signal. If the scaling of the absolute signal intensities with the number of charges can be determined, this opens the door to single-particle CD–MS on an Orbitrap mass analyzer, as both m/z and charge can be estimated for every individual ion.

To achieve experimentally the storage and thus subsequent detection of single ions in an Orbitrap, we diluted analytes to the nanomolar range, shortened the time during which ions are sampled from the continuous beam produced by ESI to the order of milliseconds, and/or down-tuned the ion-optics to further reduce ion transmission (Supplementary Notes). This is illustrated in Fig. 1b, displaying a single scan recorded for Flock house virus (FHV) particles. Many ions are detected simultaneously, although most ions have a unique m/z in the region around 41,000 m/z, with approximately 220 charges (Fig. 1c). With such a relatively high number of charges, the single-ion signals can be easily distinguished against

[1]Biomolecular Mass Spectrometry and Proteomics, Bijvoet Center for Biomolecular Research and Utrecht Institute for Pharmaceutical Sciences, University of Utrecht, Utrecht, the Netherlands. [2]Netherlands Proteomics Center, Utrecht, the Netherlands. [3]Department of Biochemistry and Molecular Biology, Center for Structural Biology, the McKnight Brain Institute, Gainesville, FL, USA. [4]Thermo Fisher Scientific (Bremen), Bremen, Germany. ✉e-mail: A.J.R.Heck@uu.nl

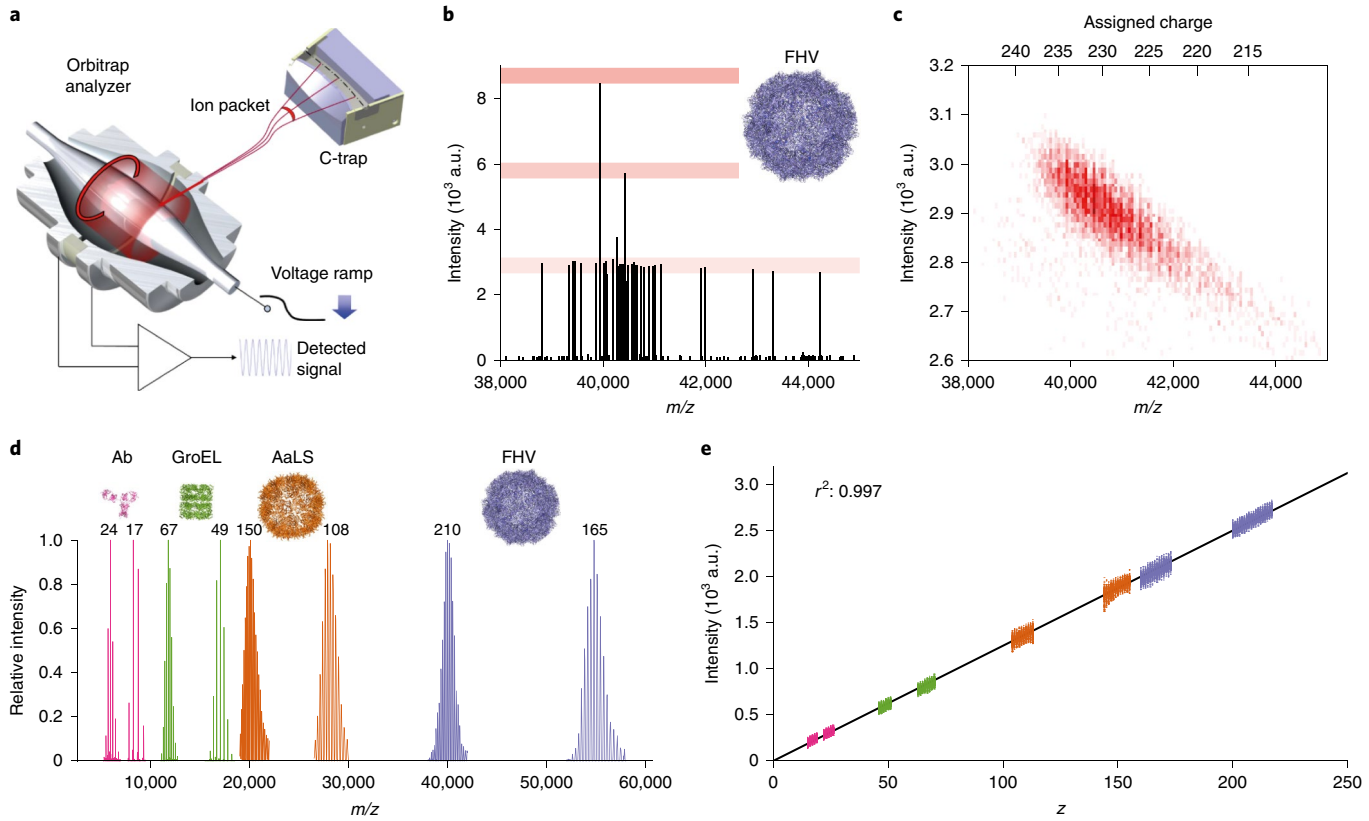

Fig. 1 | Single-ion detection and charge dependent intensity scaling with the Orbitrap mass analyzer. a, Schematic of the injection of ions from the C-trap into the Orbitrap, where they oscillate along the central electrode, inducing an image current, which is recorded and converted into a final *m/z* spectrum by Fourier transformation. **b**, A single scan showing several dozens of individual multiply charged ions of the FHV with discrete intensities around 3×10^3, highlighted by the bottom red bar. Two instances are visible where two and three ions coincide at the same frequency (*m/z*), yielding two- and threefold intensities of the single ions, highlighted by the middle and top red bars, respectively. **c**, Two-dimensional histogram of filtered single-ion signals collected over several minutes of acquisition time. The bottom *x* axis indicates the *m/z*, whereas the top *x* axis indicates the charge states. Note that the signal intensity of single FHV particles decreases with decreasing charge over the entire displayed region. **d**, Composite native MS spectra of protein assemblies measured to evaluate the scaling of single-ion intensity with charge state. Each protein assembly was analyzed with and without the addition of the charge-reducing agent triethyl ammonium acetate in the electrospray solution, resulting for each species in two mass spectra at lower and higher *m/z*, respectively. The average charge state is indicated above each spectrum; Ab, antibody. **e**, A linear regression model was fitted to 200 sampled single-ion intensities per charge state ($n=15{,}600$): Intensity = 12.521 × charge, with an r^2 of 0.997.

noise (signal to noise ratio of ~250). The small spread of single-ion intensities for individual charges confirms that most ions survive until the end of the transient. This survival rate of the ions requires a sufficiently low operating pressure of the Orbitrap (Supplementary Fig. 1). Of note, the resolution on the single-ion peaks closely follows the theoretical resolution limit of the Orbitrap (Supplementary Fig. 2). Whereas a multitude of ions is detected in every scan, almost all ions in the sample have a unique *m/z* and are thus detected and resolved as single ions. The multiplicity of ions in all scans substantially improves the duty cycle compared to measurements of a single ion at a time, as has been noted in other single-particle MS approaches[17].

To determine quantitatively how single-ion intensities scale with the number of charges, we conducted single-ion measurements on a larger set of protein complexes with well-defined masses, ranging from 150 kDa to 9.4 MDa (Fig. 1d). Each sample was sprayed from aqueous ammonium acetate, with and without the addition of the charge-reducing agent triethyl ammonium acetate[18]. The assigned charge states were compared to the single-ion intensities at the corresponding *m/z* to build a calibration curve (Supplementary Fig. 3). Figure 1e shows 200 randomly sampled ions per charge state and a linear regression model describing the single-ion intensity as a function of charge with an r^2 of 0.997. Using this linear relationship to predict the charge state of individual ions yields an r.m.s.d. of 3.5 charges (Supplementary Notes).

Next, we tested how the Orbitrap mass analyzer is capable of resolving more complex mixtures in the intensity domain. Based on single-ion intensities, we could resolve 3 MDa AaLS protein cages from 1.5 MDa ribosomal subunits that co-occur at the same *m/z* in an artificial mixture (Supplementary Fig. 4). Similarly, we were able to resolve overlapping charge states in complex mixtures of IgG oligomers (Supplementary Fig. 5). We estimate the dynamic range of our CD–MS method to be at least ~150, based on a comparison of the highest and lowest signals observed in the spectra of IgG oligomers (Supplementary Fig. 6 and Supplementary Notes).

To illustrate the benefit from the added dimension of single-ion intensity, we next analyzed IgM, which is thought to naturally exist in co-occurring variants (pentamer and hexamer)[19]. When we measured an IgM sample, recombinantly expressed without the J-chain, the Orbitrap-based CD–MS spectra clearly revealed signals from three distinct co-occurring oligomeric species. The multiple occupied glycosylation sites on IgM introduce a high grade of heterogeneity, causing broad peaks for each individual charge state, which normally cannot be resolved. Additionally, the three charge state distributions overlap extensively, resulting in a poorly resolved complex spectrum preventing charge state assignment (Fig. 2).

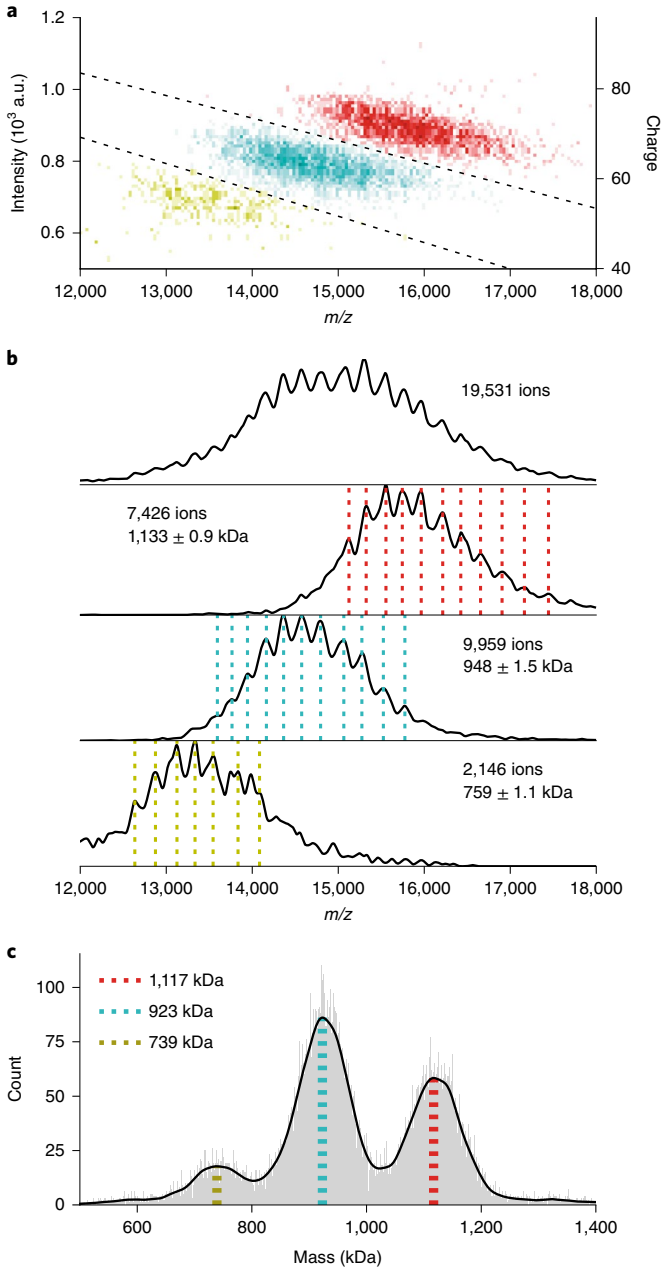

Fig. 2 | Resolving a complex mixture of IgM oligomers using single-ion intensities. a, Single-particle CD–MS of IgM oligomers. Tetrameric, pentameric and hexameric species are colored in green, cyan and red, respectively. Dotted lines indicate the margins used for the filtered subsets shown in **b**. **b**, *m/z* histogram of single-particle centroids showing the extensively overlapping charge state distributions for the three IgM oligomeric states (top). Below are shown the filtered subsets used for the charge state assignments. Dotted lines indicate top positions used for assignment and illustrate overlapping charge state series (masses are reported as mean ± s.d.). **c**, Mass histograms, calculated from ion intensities, revealing the distribution and masses of the three co-occurring species. The most abundant masses are indicated with vertical lines (same color code as in **a**,**b**) and are in close agreement with the masses determined by using conventional charge assignments as depicted in **b**.

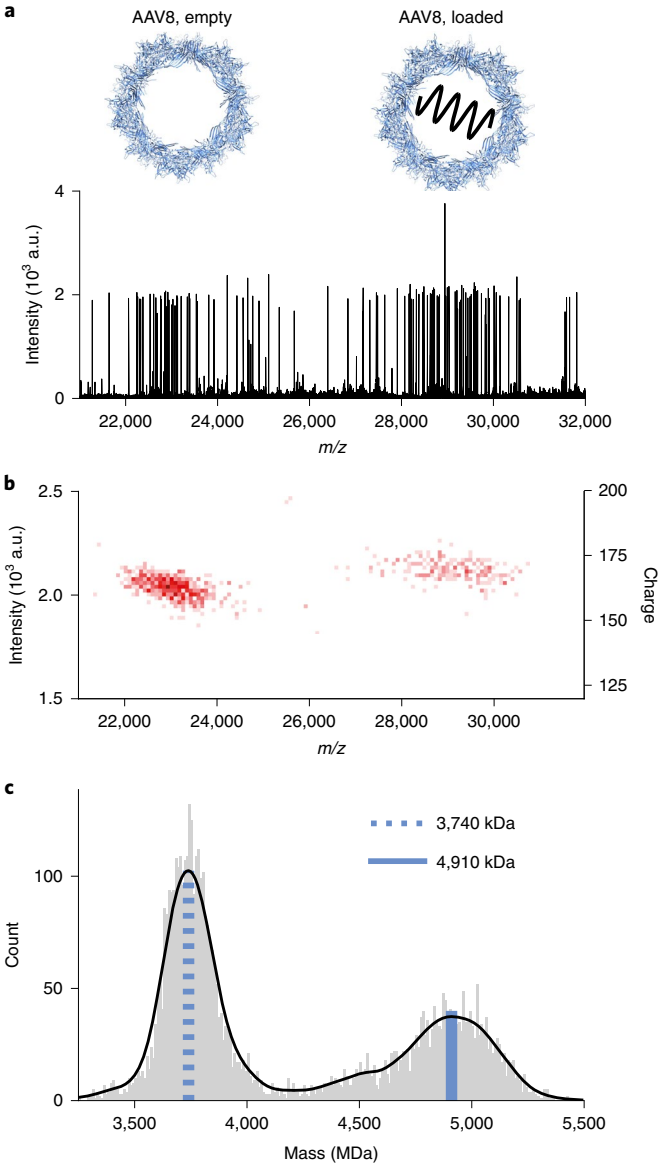

Fig. 3 | Single-particle CD–MS of co-occurring empty and genome-loaded AAV8 particles. a, Individual scan of single particles for a mixture of empty and genome-loaded AAV8 capsids. **b**, Two-dimensional histogram of filtered single-particle centroids collected over several minutes. **c**, Mass histogram for AAV8 particles directly calculated from single-ion intensities. Blue lines indicate top masses of the empty AAV8 (dotted) and the loaded AAV8 (solid) particle.

Adding the intensity dimension, signals for each species could be separated and intensity thresholds were used to filter for each oligomeric species. The resulting *m/z* histograms shown in Fig. 2b can now be used for charge assignment and quantification based on ion counts. The resulting determined molecular masses of 759, 948 and 1,133 kDa correspond to the 4-mer, 5-mer and 6-mer, and a monomer IgM mass of 189 kDa. Predicting charge and mass solely on the basis of single-particle intensity yields very similar masses for the 4-mer, 5-mer and 6-mer and a monomer mass of 185 kDa (Fig. 2c). Both monomer masses are in accordance with the IgM monomer backbone mass of 173 kDa decorated with various glycans on the six putative glycosylation sites.

The paramount application for single-particle CD–MS is in the analysis of heterogeneous complexes of which charge states cannot be resolved in conventional native MS. Similar to Pierson et al.[11], we used adeno-associated virus (AAV) as a test case as its capsid is composed of 60 copies of three different building blocks (that is, VP1, VP2 and VP3), assembled in varying stoichiometries, yielding

a wide distribution of capsid masses[20]. Genome-loaded AAV particles are even more heterogeneous, as the capsids pack a mixture of sense and antisense single-stranded DNA. To illustrate the challenges of native MS on AAV and the gains from single-particle CD–MS, we measured AAV serotype 8 (AAV8) particles with a reported average 1:1:10 (VP1:VP2:VP3) ratio and loaded with a 3.8 kB genome encoding green fluorescent protein. The large heterogeneity of these AAV particles hamper charge state assignment in conventional native MS (Supplementary Fig. 7).

A single-particle CD–MS analysis of AAV8 is presented in Fig. 3, whereby distinct distributions for empty and packaged AAV8 particles could be resolved. This analysis revealed that the empty and packaged AAV particles obtain a very similar number of charges during native ESI, despite the filled particles having a 25% higher mass. The mass of the empty particle determined by CD–MS is 3,740 kDa, deviating by just 0.3% of the expected mass. The mass of the genome-loaded particles was 4,910 kDa, yielding a genome mass of 1,170 kDa compared to the expected mass of 1,243 kDa, confirming the packaging of the complete genome without substantial defects or degradation. The reported mass deviations are well within the error margin of ~1% for megadalton particles (Supplementary Table 1) and the average mass and full width at half maximum (FWHM) (3,740 and 230 kDa, respectively) for the empty capsid are in agreement with literature[11].

In conclusion, we demonstrate the capabilities of an Orbitrap mass analyzer to directly derive the charge state of particles based on single-ion measurements. This overcomes a major bottleneck in native MS, which requires charge state resolved signals to assign charges and thus masses from *m/z* spectra. The current Orbitrap-based instruments are sufficiently sensitive enough to measure thousands of single particles in a matter of minutes, whereby the relative uncertainty on the estimated charge decreases with increasing charge state, making the technique especially suited to the analysis of large macromolecular assemblies. Moreover, Orbitrap-based single-particle CD–MS is fully compatible with all its existing tandem MS and fragmentation capabilities. We foresee a thriving and broad range of applications, especially in analyzing heterogeneous mixtures including amyloid fibrils, gene delivery vectors, highly glycosylated biotherapeutics and membrane protein complexes.

Online content

Any methods, additional references, Nature Research reporting summaries, source data, extended data, supplementary information, acknowledgements, peer review information; details of author contributions and competing interests; and statements of data and code availability are available at https://doi.org/10.1038/s41592-020-0770-7.

Received: 8 August 2019; Accepted: 5 February 2020;
Published online: 9 March 2020

References

1. Leney, A. C. & Heck, A. J. R. Native mass spectrometry: what is in the name? *J. Am. Soc. Mass Spectrom.* **28**, 5–13 (2017).
2. Mehmood, S., Allison, T. M. & Robinson, C. V. Mass spectrometry of protein complexes: from origins to applications. *Annu. Rev. Phys. Chem.* **66**, 453–474 (2015).
3. Snijder, J. & Heck, A. J. R. Analytical approaches for size and mass analysis of large protein assemblies. *Annu. Rev. Anal. Chem.* **7**, 43–64 (2014).
4. Mann, M., Meng, C. K. & Fenn, J. B. Interpreting mass spectra of multiply charged ions. *Anal. Chem.* **61**, 1702–1708 (1989).
5. Chang, H.-C. Ultrahigh-mass mass spectrometry of single biomolecules and bioparticles. *Annu. Rev. Anal. Chem.* **2**, 169–185 (2010).
6. Keifer, D. Z. & Jarrold, M. F. Single-molecule mass spectrometry. *Mass Spectrom. Rev.* **36**, 715–733 (2017).
7. Hanay, M. S. et al. Single-protein nanomechanical mass spectrometry in real time. *Nat. Nanotechnol.* **7**, 602–608 (2012).
8. Sage, E. et al. Neutral particle mass spectrometry with nanomechanical systems. *Nat. Commun.* **6**, e6482 (2015).
9. Elliott, A. G. et al. Simultaneous measurements of mass and collisional cross-section of single ions with charge detection mass spectrometry. *Anal. Chem.* **89**, 7701–7708 (2017).
10. Doussineau, T. et al. Mass determination of entire amyloid fibrils by using mass spectrometry. *Angew. Chem. - Int. Ed.* **55**, 2340–2344 (2016).
11. Pierson, E. E., Keifer, D. Z., Asokan, A. & Jarrold, M. F. Resolving adeno-associated viral particle diversity with charge detection mass spectrometry. *Anal. Chem.* **88**, 6718–6725 (2016).
12. Dominguez-Medina, S. et al. Neutral mass spectrometry of virus capsids above 100 megadaltons with nanomechanical resonators. *Science* **362**, 918–922 (2018).
13. Rose, R. J., Damoc, E., Denisov, E., Makarov, A. & Heck, A. J. R. High-sensitivity Orbitrap mass analysis of intact macromolecular assemblies. *Nat. Methods* **9**, 1084–1086 (2012).
14. Makarov, A. & Denisov, E. Dynamics of ions of intact proteins in the Orbitrap mass analyzer. *J. Am. Soc. Mass Spectrom.* **20**, 1486–1495 (2009).
15. Kafader, J. O. et al. Measurement of individual ions sharply increases the resolution of Orbitrap mass spectra of proteins. *Anal. Chem.* **91**, 2776–2783 (2019).
16. Bruce, J. E. et al. Trapping, detection, and mass measurement of individual ions in a Fourier transform ion cyclotron resonance mass spectrometer. *J. Am. Chem. Soc.* **116**, 7839–7847 (1994).
17. Sage, E. et al. Single-particle mass spectrometry with arrays of frequency-addressed nanomechanical resonators. *Nat. Commun.* **9**, 3283 (2018).
18. Pacholarz, K. J. & Barran, P. E. Use of a charge reducing agent to enable intact mass analysis of cysteine-linked antibody-drug-conjugates by native mass spectrometry. *EuPA Open Proteom.* **11**, 23–27 (2016).
19. Hiramoto, E. et al. The IgM pentamer is an asymmetric pentagon with an open groove that binds the AIM protein. *Sci. Adv.* **4**, eaau1199 (2018).
20. Snijder, J. et al. Defining the stoichiometry and cargo load of viral and bacterial nanoparticles by orbitrap mass spectrometry. *J. Am. Chem. Soc.* **136**, 7295–7299 (2014).

Methods

Native MS. Purified proteins were supplied from various sources: *E. coli* 70 S ribosome particles were purchased from New England Biolabs, trastuzumab and IgG1-RGY samples were provided by the team of J. Schuurman at Genmab (Utrecht), the IgM sample was provided by S. Rooijakkers (Medical Microbiology, UMCU), the AaLS-neg nanocontainer sample was provided by the group of D. Hilvert (ETH Zurich) and the AAV8 particles were provided by M. Agbandje-McKenna (University of Florida).

The FHV and ribosomes samples were prepared and buffer exchanged as described previously[21]. All other purified protein samples were buffer exchanged to aqueous ammonium acetate (150 mM, pH 7.5) with several concentration/dilution rounds using Vivaspin Centrifugal concentrators (9,000*g*, 4 °C). An aliquot of 1–2 µl was loaded into gold-coated borosilicate capillaries 467 (prepared in-house) for nano-ESI. Samples were analyzed on a standard commercial Q Exactive-UHMR instrument (Thermo Fisher Scientific)[21,22]. The described experiments should work in principle with any Orbitrap mass analyzer with extended mass range (branded as Exactive Plus EMR and Q Exactive-UHMR).

Instrument setting for native MS. The instrument setting required for the analysis of large assemblies such as ribosomes and FHV have been described in detail previously[21,22]. In short, ion transfer target *m/z* and detector optimization was set to 'high *m/z*' for all samples expect IgG monomers, where radio frequency amplitudes for the injection flatapole, bent flatapole, transfer multipole and higher-energy collisional dissociation (HCD) cell were set to 700, 600 and 600 V, respectively, and detector optimization was set to 'low *m/z*'. In-source trapping was enabled with desolvation voltages ranging between −50 and −200 V. The ion transfer optics (injection flatapole, inter-flatapole lens, bent flatapole and transfer multipole) were set to 10, 10, 4 and 4, except for immunoglobulins where 7, 7, 7 and 7 were used, respectively. In general, larger assemblies require higher pressure settings to allow sufficient collisional focusing in the C-trap as well as higher HCD voltages for efficient solvent adduct removal. Using xenon as a collision gas turned out to be beneficial for the analysis of high-mass ions due to the higher center-of-mass energies on collision. To maximize ion transmission, for conventional native MS experiments, pressure settings were considerably higher than for single-particle experiments. Exemplary values for ultrahigh vacuum (UHV) pressure readouts and HCD energies for xenon were 7×10^{-11} mbar and 50 V HCD for IgG, 1.5×10^{-10} mbar and 100 V HCD for IgG1-RGY hexamers, 1.5×10^{-10} mbar and 80 V HCD for GroEL, 7.5×10^{-10} mbar and 70 V HCD for AaLS-neg and 1.5×10^{-9} mbar and 200 V HCD for FHV. Spectra were recorded at set transient times between 16 and 128 ms.

Single-particle native MS data acquisition. For single-particle acquisitions, most of the tuning parameters were kept as for conventional native MS. However, pressure settings were reduced to reduce the occurrence of transient instabilities resulting in split peaks (see Supplementary Fig. 1) but had to be kept high enough to allow collisional focusing of ions in the C-trap and HCD cell. Exemplary readouts for the UHV pressure with xenon as collision gas were 3×10^{-11} mbar for IgG, 5.5×10^{-11} mbar for GroEL and ribosomes, 9×10^{-11} mbar for AaLS-neg, 1×10^{-10} mbar for IgM and IgG1-RGY hexamers, 3×10^{-10} mbar for AAV and 4×10^{-10} mbar for FHV. With nitrogen as a collision gas, exemplary UHV pressure readouts were 3×10^{-11} mbar for IgG, 4×10^{-11} mbar for GroEl, 8.5×10^{-11} mbar for IgG1-RGY hexamers and 1.5×10^{-10} mbar for AaLS-neg. Ion transmission was further attenuated by diluting the sample and reducing the injection time until spectra with singly resolved ions were acquired. Single-particle datasets were recorded with a noise level parameter set to 0, using either 512 or 1,024 ms set transients, and accumulated for 10–60 min.

Single-particle data preprocessing. Single-particle data were first converted to mzXML files using the vendor peak picking algorithm (MSConvert)[23]. To get comparable intensity values throughout different experiments all ion intensities were multiplied by their injection times in seconds. Instable transients from dephased ion signals were removed by applying an *m/z* threshold for adjacent centroids above a certain absolute intensity value of 50.The applied *m/z* threshold depended on the *m/z* region the ions populated, whereby we typically used five times the FWHM of the single-particle peaks. See Supplementary Fig. 8 for an overview of this workflow. A python class and an exemplary script for single-particle data processing are available as Supplementary Software.

Charge versus intensity regression model. Preprocessed single-ion datasets were filtered in the *m/z* and intensity dimension for the regions of interest. Centroid *m/z* positions were then binned to obtain conventional mass spectra, which were used for conventional charge assignment. Single-particle centroids were selected for each charge state based on their *m/z* position from the charge assignment. For each charge, a kernel density estimation was performed in the intensity domain and peak intensity as well as FWHM of the distribution were extracted. From each set of intensities assigned to a certain charge, 200 samples were drawn randomly within two times the FWHM of the top intensity. All sampled ion intensities and their charges were subjected to linear regression. See Supplementary Fig. 3 for an overview of the workflow.

Intensity-based charge and mass prediction. Preprocessed and filtered centroid intensities were converted into charges with the previously established regression model allowing noninteger values. Masses were then calculated from their *m/z* position using the equation $m = (m/z) \times z - z$. Masses were subjected to a kernel density estimation and most abundant masses were extracted.

Mass prediction of AAV based on *m/z* position. To estimate the mass from the *m/z* position, we fitted 76 empirical determined masses and their corresponding *m/z* positions to the equation mass (kDa) $= A \times (m/z)^B$ as reported in previous publications[24,25]. The resulting formula of mass (kDa) $= 1.63\times10^{-6}\times(m/z)^{2.14}$ was used to estimate the mass based on the peak *m/z* position for the unresolved empty and genome-loaded AAV8 particle from a spectrum recorded on a quadrupole time of flight instrument.

Reporting Summary. Further information on research design is available in the Nature Research Reporting Summary linked to this article.

Data availability

For each of the figures and supplementary figures, the underlying centroided and filtered data are available in Supplementary Data. On request, the raw data are available from the corresponding author.

Code availability

A python class and an exemplary script for single-particle data processing are available as Supplementary Software.

References

21. van de Waterbeemd, M. et al. High-fidelity mass analysis unveils heterogeneity in intact ribosomal particles. *Nat. Methods* **14**, 283–286 (2017).
22. Fort, K. L. et al. Expanding the structural analysis capabilities on an Orbitrap-based mass spectrometer for large macromolecular complexes. *Analyst* **143**, 100–105 (2017).
23. Chambers, M. C. et al. A cross-platform toolkit for mass spectrometry and proteomics. *Nat. Biotechnol.* **30**, 918–920 (2012).
24. Veesler, D. et al. Architecture of a dsDNA viral capsid in complex with its maturation protease. *Structure* **22**, 230–237 (2014).
25. Sigmund, F. et al. Bacterial encapsulins as orthogonal compartments for mammalian cell engineering. *Nat. Commun.* **9**, e1990 (2018).

Acknowledgements

We greatly appreciate the several collaborators who provided samples to us that we used in the work presented here. We acknowledge the D. Hilvert group at the ETH Zurich for providing the AaLS-neg samples, the J. Schuurman group at Genmab for providing the mutant IgG samples, the S. Rooijakkers group at the Medical Microbiology Department, University Medical Center, Utrecht, in particular P. Aerts and C. Gosselaar-de Haas, for providing the IgM samples, and the A. Routh group at the University of Texas Medical Branch, in particular E. Jaworski, for providing the FHV samples. This work was supported by the Netherlands Organization for Scientific Research through the Spinoza Award (no. SPI.2017.028) to A.J.R.H. J.S. was further supported by the NWO Gravitation project Institute for Chemical Immunology (no. 024.002.009). Additional support came through the European Union Horizon 2020 INFRAIA project Epic-XS (project no. 823839).

Author contributions

T.P.W., J.S. and A.J.R.H. conceived the project, designed the experiments and wrote the paper. A.B. and M.A.-M. prepared the AAV samples. A.A.M. advised on operation of data acquisition system and mechanisms of ion–molecule interactions in the Orbitrap analyzer for high mass ions. T.P.W. performed all experiments and processed the data. J.S. and A.J.R.H. supervised the project. T.P.W., J.S. and A.J.R.H. analyzed the results. All authors discussed the results and edited the paper.

Competing interests

A.A.M. is an employee of Thermo Fisher Scientific, the company that commercializes Orbitrap-based mass analyzers.

Additional information

Supplementary information is available for this paper at https://doi.org/10.1038/s41592-020-0770-7.

Correspondence and requests for materials should be addressed to A.J.R.H.

Peer review information Allison Doerr was the primary editor on this article and managed its editorial process and peer review in collaboration with the rest of the editorial team.

nature research

Corresponding author(s): A.J.R. Heck

Last updated by author(s): Feb 3, 2020

Reporting Summary

Nature Research wishes to improve the reproducibility of the work that we publish. This form provides structure for consistency and transparency in reporting. For further information on Nature Research policies, see Authors & Referees and the Editorial Policy Checklist.

Statistics

For all statistical analyses, confirm that the following items are present in the figure legend, table legend, main text, or Methods section.

n/a	Confirmed	
☒	☐	The exact sample size (*n*) for each experimental group/condition, given as a discrete number and unit of measurement
☒	☐	A statement on whether measurements were taken from distinct samples or whether the same sample was measured repeatedly
☒	☐	The statistical test(s) used AND whether they are one- or two-sided *Only common tests should be described solely by name; describe more complex techniques in the Methods section.*
☐	☒	A description of all covariates tested
☐	☒	A description of any assumptions or corrections, such as tests of normality and adjustment for multiple comparisons
☐	☒	A full description of the statistical parameters including central tendency (e.g. means) or other basic estimates (e.g. regression coefficient) AND variation (e.g. standard deviation) or associated estimates of uncertainty (e.g. confidence intervals)
☒	☐	For null hypothesis testing, the test statistic (e.g. *F*, *t*, *r*) with confidence intervals, effect sizes, degrees of freedom and *P* value noted *Give P values as exact values whenever suitable.*
☒	☐	For Bayesian analysis, information on the choice of priors and Markov chain Monte Carlo settings
☒	☐	For hierarchical and complex designs, identification of the appropriate level for tests and full reporting of outcomes
☒	☐	Estimates of effect sizes (e.g. Cohen's *d*, Pearson's *r*), indicating how they were calculated

Our web collection on statistics for biologists contains articles on many of the points above.

Software and code

Policy information about availability of computer code

Data collection	MS tune QE-UHMR 2.11
Data analysis	ProteoWizard 3, Python 3.6

For manuscripts utilizing custom algorithms or software that are central to the research but not yet described in published literature, software must be made available to editors/reviewers. We strongly encourage code deposition in a community repository (e.g. GitHub). See the Nature Research guidelines for submitting code & software for further information.

Data

Policy information about availability of data

All manuscripts must include a data availability statement. This statement should provide the following information, where applicable:

- Accession codes, unique identifiers, or web links for publicly available datasets
- A list of figures that have associated raw data
- A description of any restrictions on data availability

The filtered data that support the findings of this study are available as csv files. Raw data (several Gb's) are upon request available from the corresponding author .

Field-specific reporting

Please select the one below that is the best fit for your research. If you are not sure, read the appropriate sections before making your selection.

☒ Life sciences ☐ Behavioural & social sciences ☐ Ecological, evolutionary & environmental sciences

Life sciences study design

All studies must disclose on these points even when the disclosure is negative.

Sample size	Sampling of 200 ions per charge state for linear regression as described in the method section
Data exclusions	Single particle data was filtered for split ion signal as described in the method section
Replication	Charge vs. Intensity calibration was replicated as shown in supplementary figure 9
Randomization	No randomization was applicable since no organization in experimental groups
Blinding	No blinding was applicable since no organization in experimental groups

Reporting for specific materials, systems and methods

We require information from authors about some types of materials, experimental systems and methods used in many studies. Here, indicate whether each material, system or method listed is relevant to your study. If you are not sure if a list item applies to your research, read the appropriate section before selecting a response.

Materials & experimental systems

n/a	Involved in the study
☒	☐ Antibodies
☒	☐ Eukaryotic cell lines
☒	☐ Palaeontology
☒	☐ Animals and other organisms
☒	☐ Human research participants
☒	☐ Clinical data

Methods

n/a	Involved in the study
☒	☐ ChIP-seq
☒	☐ Flow cytometry
☒	☐ MRI-based neuroimaging